A PMU-Based State Estimator For Networks Containing VSC-HVDC links

Wei Li
School of Electrical Engineering
KTH Royal Institute of Technology
Stockholm, Sweden
Email: wei3@kth.se

Luigi Vanfretti
KTH Royal Institute of Technology, Stockholm, Sweden
Email: luigiv@kth.se
Statnett SF, Research & Development, Oslo, Norway
Email: luigi.vanfretti@statnett.no

***Abstract*—This paper presents a PMU-based state estimation algorithm that considers the presence of voltage source converter-based high voltage direct current (VSC-HVDC) links. The network model of a VSC-HVDC link with its control modes is developed and then combined with an AC model to accomplish a hybrid AC/DC network model. The measurement model in this algorithm considers the properties of PMU measurements, thus separating the network model with measurements. Additionally, DC link measurements are assumed to be sampled synchronously, time-stamped and reported at the same rate as PMU measurements. Then, by applying the nonlinear weighted least squares (WLS) algorithm, a PMU-based state estimator can solve for both AC and DC states simultaneously. To validate the algorithm, a simulation study for a 6-bus hybrid AC/DC test system is shown in this paper.**

I. Introduction

VSC-based HVDC systems have been successfully exploited in various project among the world. Compared to the classic HVDC technology, often referred to as current source converter line commutated (CSC-LCC), VSC-HVDC technology offers a key advantage of independent control of active and reactive powers, together with additional benefits in control flexibility and reliability [1]. Up to date, VSC-HVDC is widely and effectively applied to interconnected remote generation plants, isolated remote loads, metropolitan areas, and offshore bays, etc [2].

However, at the same time, this state-of-art technology brings many challenges in power system operation. Improvements in power system monitoring are required in order to adapt to these challenges. One important aspect is power system state estimation (PSSE). PSSE is a process that determines the state of a network by using measurements and a model of the grid. With a proper redundancy level, state estimation (SE) can eliminate the effect of bad data and produce reliable state estimates in order to help operators monitor the grid and to support other functions in Energy Management Systems (EMS) [3]. Taking VSC-HVDC into account of PSSE was investigated in few articles, e.g.[4]; however, the applied algorithm was based on conventional SE.

Conventional SE is performed using a combination of measurements provided by a supervisory control and data acquisition (SCADA) system, and pseudo-measurements. SCADA system provides conventional SEs with asynchronous measurements every 2 to 10 seconds, which limits the speed at which the state estimator can be executed. Recently, phasor measurement units (PMUs) have been implemented to complement the conventional metering devices and bring additional monitoring measurements to the EMS. PMUs provide GPS time-synchronized measurements at a rate of 30-50 samples per second. Hence, a PMU data-based state estimator [5]-[7] can follow the trajectory of the power system and sanitize data quickly to support other applications.

To adapt to the update on meter facilities, a PMU-based state estimation algorithm, which has been demonstrated in [5] by the authors, is applied. A comprehensive VSC-HVDC model with vector-current control scheme [8]-[11] for SE purpose is proposed in this paper. Furthermore, this model is combined with a unified AC network model to achieve hybrid AC/DC network SE.

The remainder of this paper is organized as follows. First, in Section II, different fragments of a hybrid AC/DC network model are presented, including a unified AC network branch model, a VSC station model with different control modes, and a point-to-point VSC-HVDC link model. Second, Section III briefly introduces the applied PMU-based state estimation algorithm together with its measurement model. Finally, simulation results are shown in Section IV, and conclusions and future work are discussed in Section V.

II. Hybrid AC/DC network model

A. Unified AC network branch model

PMUs measure voltage phasors $\tilde{\mathbf{V}}$ at buses where PMUs installed and current phasors $\tilde{\mathbf{I}}$ on lines adjacent to the buses. Directly using $\tilde{\mathbf{V}}$ and $\tilde{\mathbf{I}}$ into network model could significantly reduce the nonlinearity of the network model and the corresponding Jacobian matrix. Based on these measured variables, a unified AC network branch model is proposed, which takes series impedances, shunt admittances, and transformers into account. Figure 1 shows its structure.

The subscript $\boldsymbol{f}$ denotes the bus where current flows from and $\boldsymbol{t}$ is the bus where current flows to. AC lines are represented by series impedance vector Z and shunt admittance Y in per unit. A transformer is represented by the off-nominal tap ratio $a:1$. In the case of phase shifting transformers, a is a complex number. The model in Fig. 1 can be formulated in

978-1-4673-8040-9/15/$31.00 ©2015 IEEE

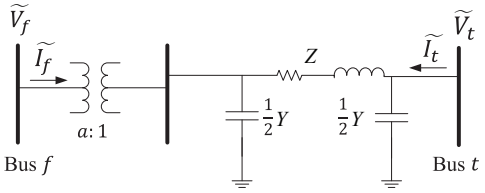

Fig. 1. AC line with transformer

terms of the *ABCD* constants as:

$$\begin{bmatrix} \widetilde{\mathbf{V_f}} \\ \widetilde{\mathbf{I_t}} \end{bmatrix} = \begin{bmatrix} \mathbf{a}(1+\frac{\mathbf{ZY}}{2}) & \mathbf{aZ} \\ \frac{\mathbf{Y}}{\mathbf{a}^*}(1+\frac{\mathbf{ZY}}{4}) & \frac{1}{\mathbf{a}^*}(1+\frac{\mathbf{ZY}}{2}) \end{bmatrix} \begin{bmatrix} \widetilde{\mathbf{V_t}} \\ \widetilde{\mathbf{I_t}} \end{bmatrix}. \quad (1)$$

Compared to the conventional SE network model, which adopts power flow network equations, this model uses Kirchhoff's laws with voltage and current phasors so as to significantly reduce the nonlinearities, as well as to reduce the computation burden of the numerical solution algorithms.

B. VSC station model

To match PMUs measurements in AC systems, DC measurement units (DMUs) could be easily implemented by extending the functionalities of the acquisition systems used in converter stations to gather DC measurements. Based on the knowledge that switching frequency of transistors or thyristors in VSC is extremely high and so is the control response, DMUs should be capable to provide high speed and GPS time-synchronized measurements, at least not slower than PMUs.

A basic diagram of a VSC station is shown in Fig. 2. Basic components in a VSC station contain an AC/DC converter, DC capacitor(s), a phase reactor, a transformer and filter(s). The converter requires self-commutating switches, such as gate turn on thyristors (GTO) or insulated-gate bipolar transistors (IGBT), which have a turn-on and turn-off capability. The DC capacitor in the DC side strongly maintains the required voltage. However, in reality, DC voltage exists ripples due to harmonic currents in the DC circuit generated during VSC operation. The interface transformer and phase reactors are installed to reduce the fault current and the harmonic current content in the AC current, and enable the control of active and reactive power flow. The AC filter aims to filtering the high-order harmonics created by the commutation valve switching process [1].

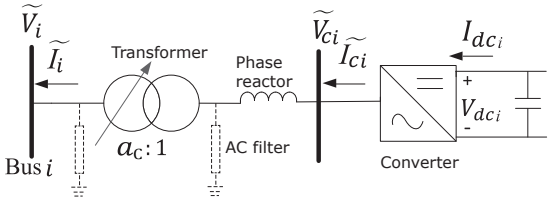

Fig. 2. Basic diagram of a VSC station [1]

Based on the time-scale at which PMUs report data and at which the SE is executed, the VSC station model can be simplified by replacing the AC filter and phase reactor with a series impedance of z_i. Thus, the AC line connecting bus i and VSC station i can be represented by the AC branch model with $Y = 0$ to build up the relation between bus voltage and current phasors with converter voltage and current phasors. Hence, it is formulated as:

$$\begin{cases} 0 = \widetilde{V_{ci}} - \frac{1}{a_c}\widetilde{V_i} - a_c^*\widetilde{I}_i z_i \\ 0 = \widetilde{I_{ci}} - a_c^*\widetilde{I}_i \end{cases} \quad (2)$$

To exploit the relation between converter voltage and current with DC voltage and current, the converter and its operation have to be modeled. There are mainly two types of VSC models: the detailed model and the averaged value model (AVM). The detailed model includes semiconductor devices; additionally, it requires a clear definition of the converter topology, such as a two-level three-phase bridge topology or a multi-level modulation topology. All of these configurations and specifications are suitable for electromagnetic transient simulations, but not necessary for VSC modeling in PMU-based SE. This is because SEs generally engage to large systems, thus, time consuming calculations in a detailed model have to be abstained. Instead, the AVM avoids distinguishing among different switching levels and modulation types. It exclusively represents the fundamental frequency voltage and current components.

An AVM model can be represented by a combination of controllable three-phase AC voltage sources connected to the AC circuit and a controllable current source connected to the DC circuit. These three phase voltages are controlled by their respective modulation indexes, namely: m_a, m_b and m_c. Therefore, the relationship between the AC and DC circuits can be formulated as:

$$\begin{cases} v_{ci}^a = m_a V_{DCi} \\ v_{ci}^b = m_b V_{DCi} \\ v_{ci}^c = m_c V_{DCi}. \end{cases} \quad (3)$$

Besides, regardless of the power flow direction, the power consumption on one side must be always equal to the power injection from the other side. Thus,

$$I_{DCi} = \frac{v_{ci}^a i_{ci}^a + v_{ci}^b i_{ci}^b + v_{ci}^c i_{ci}^c}{V_{DCi}} = m_a i_{ci}^a + m_b i_{ci}^b + m_c i_{ci}^c. \quad (4)$$

All the AC variables in (3) and (4) use lowercase letters, which indicates they are instant variables; V_{DCi} and I_{DCi} use uppercase letters because when using the AVM DC variables are relatively constant without considering the harmonics. Note that if the DC side connection is bipolar, which is very common in applications where overhead lines are used to transmit power, all the right sides of the equations in (3) and (4) need to be divided by 2.

On the other hand, SEs utilize positive sequence model instead of three-phase model. Therefore, (3) and (4) need to be rewritten as:

$$\begin{cases} 0 = \dfrac{M_{vi}}{2} V_{DCi} - |\widetilde{V_{ci}}| \\ 0 = \dfrac{I_{DCi}}{M_{ci}\cos(\theta_{ci} - \delta_{ci})} - |\widetilde{I_{ci}}|. \end{cases} \quad (5)$$

In (5), $\widetilde{V_{ci}}$ and $\widetilde{I_{ci}}$ are the voltage and current phasors at the AC side of converter i. They can be computed from the positive-sequence component of the three-phase input signal at the fundamental frequency. θ_{ci} and δ_{ci} are the voltage and current angles, respectively. M_{vi} is the modulation index which is defined in this paper as the ratio of the root-mean-square (rms) value of the modulating wave (i.e. positive-sequence component of the AC voltage at the converter), and the peak value of the carrier wave (i.e. the DC voltage). M_{ci} denotes the ratio of the peak value of the carrier wave (i.e. the DC current), and the projection of AC current rms value on the AC voltage vector. In ideal conditions, e.g., omitting high frequency harmonic components and VSC losses, M_{ci} equals to M_{vi}. However, in reality, there is a minor discrepancy between them. Therefore, by tuning their values based on measurement data, more accurate values for each specific link can be attained.

Equation (5) holds under the assumption that all variables are in true values. If per-unit values are used, then the equation needs to be modified by considering all the base ratings.

C. VSC control modes

Generally, VSCs contain a two-level control strategy. The high-level control provides accurate voltage reference for each phase of AVM (or for each sub-module of a detailed model), so as to maintain the control variables within an acceptable range. Among the high-level control scheme, vector-current control has been successfully applied on several VSC-HVDC link installations.

Inside vector-current control, it has a two-loop control scheme, referred to as the outer control loop and the inner control loop. The outer control loop transfers the VSC control references, i.e. P^{ref}, Q^{ref}, V_{DC}^{ref} or V_{ac}^{ref}, into converter current references in d and q coordinate as $\mathbf{i_{dq}^{ref}} = (i_d^{ref}\ i_q^{ref})^T$. The inner control loop transfers the converter current references $\mathbf{i_{dq}^{ref}} = (i_d^{ref}\ i_q^{ref})^T$ into converter bridge voltage as $\mathbf{v_{dq}^{ref}} = (v_d^{ref}\ v_q^{ref})^T$. Then, they are transformed to three-phase quantities, which are the converter voltage references for the three phases.

At last, a low-level control scheme is utilized, such as pulse width modulation (PWM) algorithm, to regulate the switching signal generation by using the voltage references provided by the high-level control and thus provides switching pulses for valves. This is out of the scope of this paper because in an AVM the converter is represented by voltages sources for three phases, no switching devices being included. More details can be found in [10], [11] and [12].

Depending on the operation mode, reference i_d^{ref} can be determined from either the active power reference or the DC voltage reference. Similarly, reference i_q^{ref} can be determined from either the reactive power reference or the AC voltage reference. For each VSC station, only one i_d^{ref} and only one i_q^{ref} are allowed to be implemented. Thus, a choice of d control reference (choosing between P_{ref} and V_{DC}^{ref}), and q control reference (choosing between Q^{ref} and V_{ac}^{ref}) has to be made. Therefore, control modes for a VSC station are formulated as follows:

$$\begin{cases} 0 = C_P * (|\widetilde{V_i}| * |\widetilde{I_i}| * \cos(\theta_i - \delta i) - P^{ref}) + C_{Vd} * (V_{DCi} - V_{DCi}^{ref}) \\ 0 = C_Q * (|\widetilde{V_i}| * |\widetilde{I_i}| * \sin(\theta_i - \delta i) - Q^{ref}) + C_{Va} * (V_i - V_i^{ref}), \end{cases} \tag{6}$$

where $\mathbf{C_P}$, $\mathbf{C_{Vd}}$, $\mathbf{C_Q}$ and $\mathbf{C_{Va}}$ are the control mode indexes. $\mathbf{C_i} = 1$ indicates the corresponding control mode is activated, otherwise $\mathbf{C_i} = 0$ indicates the corresponding control mode is out of operation.

Note that to include the control modes into the state estimator, only the equilibrium condition of a system is necessary, which means controlled variables are presumed to be equal to the references. There are two reasons to make this assumption. First, the state estimator model does not include differential equations to represent system dynamics. Nevertheless, fast rate of the PMU-based SE will compensate for it as the Kirchhoff's laws of the network model should hold at each measurement snapshot. Second, vector-current control is rather fast and robust, particularly, it is facilitated with many saturation limiters to protect hardware from being damaged by peak currents after perturbation occur. Hence, the discrepancy of controlled variables is within a small range even during a perturbation, which would not greatly detract the accuracy of the proposed control modes equations. Therefore, including control modes into the state estimator improves its robustness and accuracy, without sacrificing the computational burden and execution speed.

In a summary, by combining Equ. (2), (5) and (6), a VSC station model with different control modes can be obtained as:

$$\begin{cases} 0 = \widetilde{V_{ci}} - \frac{1}{a_c}\widetilde{V_i} - a_c^*\widetilde{I_i} z_i \\ 0 = \widetilde{I_{ci}} - a_c^*\widetilde{I_i} \\ 0 = \dfrac{M_{vi}}{2} V_{DCi} - |\widetilde{V_{ci}}| \\ 0 = \dfrac{I_{DCi}}{M_{ci}\cos(\theta_{ci} - \delta ci)} - |\widetilde{I_{ci}}| \\ 0 = C_P * (|\widetilde{V_i}| * |\widetilde{I_i}| * \cos(\theta_i - \delta i) - P^{ref}) + C_{Vd} * (V_{DCi} - V_{DCi}^{ref}) \\ 0 = C_Q * (|\widetilde{V_i}| * |\widetilde{I_i}| * \sin(\theta_i - \delta i) - Q^{ref}) + C_{Va} * (V_i - V_i^{ref}) \end{cases} \tag{7}$$

D. Point-to-point VSC-HVDC link model

A single VSC has limited applications in reality, which may operate as a shunt-type FACTS device, such as a static synchronous source series compensator (SSSC) [13]. A more common application of a VSC is the point-to-point VSC-HVDC link, as shown in Fig. 3. Two VSC stations are connected through a long distance DC cable. Since the VSC is a bidirectional converter, it enables to change the power flow direction. One VSC acts the rectifier and the other one will act as an inverter, depending on the power flow control references and settings.

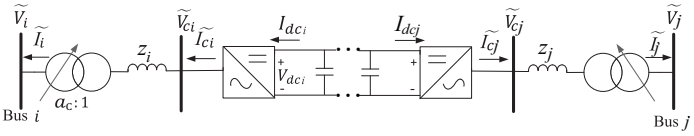

Fig. 3. A point-to-point VSC-HVDC link model

For the point-to-point VSC-HVDC link, each converter can be modeled as a VSC station as in (7). Additionally, the DC link can be modeled with a resistor. Thus,

$$\begin{cases} 0 = V_{DCi} - V_{DCj} + I_{DCi} * R_{DC} \\ 0 = I_{DCi} + I_{DCj} \end{cases} \tag{8}$$

The control strategy for a point-to-point VSC-HVDC link needs to take both converter stations into account. Since only one DC voltage reference can be used in the link, either rectifier or inverter would be assigned to control DC voltage, and the other one has to choose the active power control for d axis control. With respect to the q axis control, both stations can be operated under AC voltage control or reactive power control. Moreover, from each converter's point of view, (6) still holds for d and q axis controls.

Therefore, by combining (7) and (8) the point-to-point VSC-HVDC link model can be formulated.

III. Measurement Model and PMU-based State Estimation Algorithm

The conventional SE formulation for nonlinear systems is based on the nonlinear measurement model [3]:

$$\mathbf{z} = \mathbf{h}(\mathbf{x}) + \mathbf{e}, \tag{9}$$

where $\mathbf{z} \in \mathbb{R}^m$ is the measurement vector, $\mathbf{x} \in \mathbb{R}^n$ is the state vector, $\mathbf{h} : \mathbb{R}^n \to \mathbb{R}^m$ is a nonlinear function relating measurements to states, and $\mathbf{e} \in \mathbb{R}^m$ is the measurement error vector, which is assumed to have a normal distribution, i.e., $\mathbf{e} \sim \mathcal{N}(0, \mathbf{R_z})$. $\mathbf{R_z}$ denotes the corresponding measurement covariance matrix.

However, when PMUs are used for data acquisition, the state variables can be measured directly ($\widetilde{\mathbf{V}}$, $\widetilde{\mathbf{I}}$ phasors). A direct consequence is that the choice of state variables to be included in $\mathbf{z}$ (see (9)) can not be uniquely determined. Therefore, the choice will affect the estimation accuracy of different states. Any variable chosen to be $\mathbf{z}$ in the measurement model will lose the corresponding element in the Jacobian matrix. In other words, the network model and corresponding Jacobian matrix lose their uniqueness. Based on above consideration, a different measurement model is needed to separate the measurement variables from the network model. The proposed measurement model is formulated as follows:

$$\mathbf{e} = \begin{bmatrix} \mathbf{h}(\mathbf{x}) \\ \mathbf{x} \end{bmatrix} - \begin{bmatrix} \mathbf{0} \\ \mathbf{z} \end{bmatrix}, \tag{10}$$

where $\mathbf{h} : \mathbb{R}^n \to \mathbb{R}^k$, k is the number of network model equations. $\mathbf{h}(\mathbf{x})$ is the "pure" network model for hybrid AC/DC systems without measurements involved. This separation strategy enables to safeguard the network model from missing measurements. Although it increases the measurement model's dimension, its high sparsity will significantly compensate the computation burden.

The performance index $J(\mathbf{x})$ based on the proposed measurement model is expressed as follows:

$$J(\mathbf{x}) = \frac{1}{2}\left[\sum_{i=1}^{k}\left(\frac{h_i(\hat{\mathbf{x}})}{\sigma_i}\right)^2 + \sum_{j=1}^{m}\left(\frac{\hat{x_j} - z_j)}{\sigma_j}\right)^2\right], \tag{11}$$

where the inverse of σ_i^2 is the weighting of the i-th network equation in WLS, the inverse of σ_j^2 is the weighting of j-th measurement. In order to minimize the estimation error, the performance index $J(\mathbf{x})$ should be minimized. This can be achieved when σ_i equals to the standard variance of the i-th network model equation error and σ_j equals to the standard variance of the j-th measurement.

Both Gauss-Netwon and Newton-Raphson methods can be used to solve the nonlinear WLS problem, which has been described in literature, e.g., [3].

IV. Simulation Study

A 6-bus hybrid AC/DC test system is applied to validate the proposed VSC models and SE algorithm. The diagram of the 6-bus system with an embedded point-to-point VSC-HVDC link is shown in Fig. 4. Synthetic measurements used for SE computations were obtained by running a time-domain simulation of a three-phase model in `MATLAB/Simulink`, and 20 us is selected as the step-size. For this test, all the weightings for network equations and measurements were presumed to be 1, and full measurement observability was satisfied, in order to avoid influences of weightings and measurement redundancy on SE. A line breaker located on line 4, between bus 4 and 6, was opened at $t = 2$ s and after three cycles it was re-closed at $t = 2.06$ s. Figure 5 shows partial SE computation results for multiple snapshots.

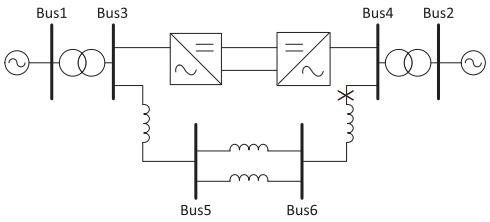

Fig. 4. 6-bus hybrid AC/DC system

As shown in Fig. 5, the residuals between estimation results and "true values" (obtained from `MATLAB/Simulink` simulation and then processed to mimic phasor data) are maintained around 10^{-3}, which is reasonable in the presence of measurement noises and ambiguous modelings between `MATLAB/Simulink` model and state estimator model. This simulation study mimics a realistic condition that may be found in field installations.

On the other hand, when the system was subject to a perturbation, the estimation residuals increased to 10^{-1}. This is because the topology of the system changed when the perturbation occurred; however, the SE model remained the same and was not adapted to the change accordingly. This indeed explains why estimation residuals increased at the instance when the breaker was opened and then came back to a normal level after the breaker was closed. Nevertheless, the estimation explicitly followed the dynamic changes during the perturbation. Topology processing or network model updating is out of the scope of this paper, but will be carried out in the

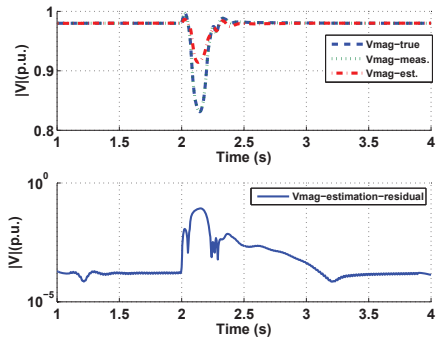

(a) Voltage magnitudes at Bus 4 for multiple snapshots

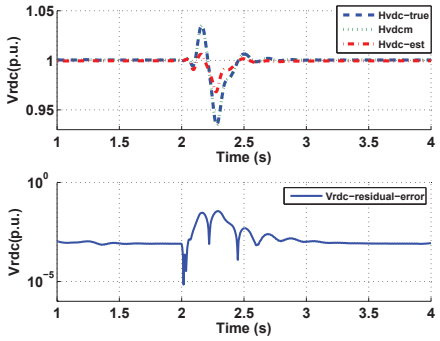

(b) DC voltage at rectifier side for multiple snapshots

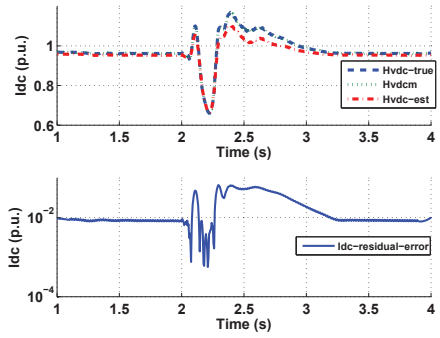

(c) DC current for multiple snapshots

Fig. 5. PSE for the 6-bus hybrid AC/DC system for multiple snapshots

future work in order to obtain better estimation results during dynamic changes. The work in [14] is a good starting point.

V. Conclusion and Discussion

A PMU-based state estimator for networks containing VSC-HVDC links has been introduced. By applying Kirchhoff's laws, the proposed network model simplifies the nonlinearities of the conventional network model. In particular, network models for a VSC-HVDC station and a point-to-point VSC-HVDC link for the PMU-based SE are developed. Different control modes are also included to enrich network information. Moreover, network model is separated from measurements in the applied measurement model in order to protect the network model from missing measurements. All the AC and DC states are simultaneously considered to solve nonlinear WLS problem. After posing the network model and measurement model for state estimator algorithm, computation results for a 6-bus hybrid AC/DC test system are presented.

The proposed state estimator significantly reduces the nonlinearities of both network model and measurement model, which dramatically decreases computation load and enables SEs for larger systems. Although estimation accuracy during system dynamic changes decreases compared to that for steady state, it is expected to be greatly improved as long as the network model performs real-time update within each measurement snapshot. Therefore, future work will focus on including network model update or topology processing into the state estimator.

Acknowledgment

The authors gratefully acknowledge the contributions of Prof. Joe H. Chow of the Rensselaer Polytechnic Institute in the form of valuable comments and suggestions to improve this paper.

References

[1] J. Arrillaga, Y. H. Liu, N. R. Watson, *Flexible Power Transmission: The HVDC Options*. New York: John Wiley & Sons, Inc., 2007.

[2] N. Rlourentzou, V. G. Agelidis, and G. D. Demetriades, "VSC-Based HVDC Power Transmission Systems: An Overview", *IEEE Trans. Power Elec.*, vol. 24, no. 3, Mar. 2009.

[3] A. Monticelli, *State Estimation in Electric Power Systems–A Generalized Approach*. Massachusetts: Kluwer Academic Publishers, 1999.

[4] A. V. Jaén, E. Acha, and A.G.Expósito, "Voltage Source Converter Modeling for Power System State Estimation: STATCOM and VSC-HVDC", *IEEE Trans. Power Syst.*, vol. 23, no. 4, Nov. 2008.

[5] W. Li, and L. Vanfretti, "Inclusion of Classic HVDC links in a PMU-Based State Estimator," *IEEE PES General Meeting*, July 2014.

[6] L. Vanfretti, J. H. Chow, S. Sarawgi, B. Fardanesh, "A Phasor-Data-Based State Estimator Incorporating Phase Bias Correction," *IEEE Trans. Power Syst.*, vol. 26, no. 1, pp. 111-119, Feb. 2011.

[7] S. G. Ghiocel, J. H. Chow, *et al.*, "Phasor-Measurement-Based State Estimation for Synchrophasor Data Quality Improvement and Power Transfer Interface Monitoring," *IEEE Trans. Power Syst.*, vol. 29, no. 2, pp. 881-888, March 2014.

[8] L. Harnefors and H.-P. Nee, "Model-based current control of AC machines using the internal model control method, *IEEE Trans. Industry App.*, vol. 34, no. 1, pp. 133141, 1998.

[9] L. Zhang, "Modeling and control of VSC-HVDC links connected to weak ac systems, Ph.D. dissertation, KTH, Electrical Machines and Power Electronics, 2010.

[10] R. Rogersten, L. Vanfretti, W. Li, L. Zhang, and P. Mitra, "A Quantitative Method for the Assessment of VSC-HVdc Controller Simulations in EMT Tools", *IEEE ISGT Europe*, Oct, 2014.

[11] M. R. Hasan, L. Vanfretti, and W. Li, "Generic High Level VSC-HVDC Grid Controls and Test Systems for Offline and Real Time Simulation", *Electric Power Quality and Supply Reliability*, Jun., 2014.

[12] L. Vanfretti, N. A. Khan, W. Li, M. R. Kasan, and A. Haider, "Generic VSC and Low Level Switching Control Models for Offline Simulation of VSC-HVDC Systems", *Electric Power Quality and Supply Reliability*, June, 2014.

[13] F. A. R. Al Jowder and B. T. Ooi, "VSC-HVDC station with SSSC characteristics, *IEEE Trans. Power Electron.*, vol. 19, no. 4, pp. 1053-1059, Jul. 2004.

[14] M. Farrokhabadi, and L. Vanfretti, "An efficient automated topology processor for state estimation of power transmission networks", *Electric Power Systems Research*, vol. 106, pp. 188 - 202, Jan. 2014.